Towards mapping the diversity of canopy structure from space with GEDI

Environmental Research Letters

Towards mapping the diversity of canopy structure from space with GEDI

To cite this article before publication: Fabian D. Schneider *et al* 2020 *Environ. Res. Lett.* in press https://doi.org/10.1088/1748-9326/ab9e99

Towards mapping the diversity of canopy structure from space with GEDI

Fabian D. Schneider[a,*], Antonio A. Ferraz[a], Steven Hancock[b,c], Laura I. Duncanson[c], Ralph O. Dubayah[c], Ryan P. Pavlick[a], David S. Schimel[a]

[a] *Jet Propulsion Laboratory, California Institute of Technology, 4800 Oak Grove Drive, Pasadena, CA 91109, USA*

[b] *Institute of Geography, University of Edinburgh, Alexander Crum Brown Road, Edinburgh, EH9 3FF, UK*

[c] *Department of Geographical Sciences, University of Maryland, 7251 Preinkert Drive, College Park, MD 20742, USA*

[*]corresponding author: fabian.schneider@jpl.nasa.gov

keywords: biodiversity | spaceborne lidar | ALS | functional traits | remote sensing

Abstract Plant biodiversity supports life on Earth and provides a range of important ecosystem services, but is under severe pressure by global change. Structural diversity plays a crucial role for carbon, water and energy cycles and animal habitats. However, it is very difficult to map and monitor over large areas, limiting our ability to assess the status of biodiversity and predict change. NASA's Global Ecosystem Dynamics Investigation (GEDI) provides a new opportunity to measure 3D plant canopy structure of the world's temperate, Mediterranean and tropical ecosystems, but its potential to map structural diversity is not yet tested. Here, we use wall-to-wall airborne laser scanning (ALS) to simulate GEDI data ($GEDI_{sim}$) over 7380 km^2 in the southern Sierra Nevada mountains in California, and evaluate how well GEDI's sampling scheme captures patterns of structural diversity. We evaluate functional richness and functional beta diversity in a biodiversity hot spot. $GEDI_{sim}$ performed well for trait retrievals (r^2 = 0.68) and functional richness mapping (r^2 = 0.75) compared to ALS retrievals, despite lower correlations in complex terrain with steep slopes. Functional richness patterns were strongly associated with soil organic carbon stocks and density as well as variables related to water availability, and could be appropriately mapped by $GEDI_{sim}$ with and without cloud cover. Functional beta diversity was more strongly related to local changes in topography and more challenging to map, especially with decreasing sampling density. The reduced number of $GEDI_{sim}$ shots when simulating cloud cover lead to a strong overestimation of beta diversity and a reduction of r^2 from 0.64 to 0.40 compared to ALS. The ability to map functional richness has been demonstrated with potential application at continental scales that could be transformative for our understanding of large-scale patterns of plant canopy structure, diversity and potential links to animal diversity, movement and habitats.

Introduction

NASA's Global Ecosystem Dynamics Investigation (GEDI) is a spaceborne lidar sensor designed specifically for measuring Earth surface structure including detailed information about 3D canopy structure of terrestrial vegetation (Dubayah et al., 2020). GEDI was successfully launched and installed on the International Space Station (ISS) in December 2018 and started its official operational data acquisition in March 2019. GEDI provides measurements of the terrestrial Earth surface between 51.6° north and south, following the ISS path, over a minimum planned mission length of two years. Besides the goal of providing a contiguous large-scale biomass map of the world's temperate and tropical forests at 1 km spatial resolution, GEDI provides a range of products that characterize 3D vegetation canopy structure (Dubayah et al., 2020). The full-waveform sampling of GEDI allows the derivation of vertically resolved information related to canopy height, density and layering (Hancock et al., 2019; Marselis et al.,

2019). Using this potential to map plant structural diversity can reveal large-scale biodiversity patterns and inform macroecology through its links to animal habitats, movement and diversity. However, since GEDI is a sampling instrument sending laser pulses that reach 25 m diameter on the ground, spaced at 60 m along track and 600 m across track, it is not yet tested to what degree GEDI can capture large-scale diversity patterns and how GEDI observed structural traits relate to established measurements from airborne laser scanning (ALS) acquisitions.

ALS combines light detection and ranging (lidar) with airborne scanning of actively emitted laser beams, resulting in a geo-located measurement of returned laser energy that can be discretized into a 3D point cloud (Wehr & Lohr, 1999). It has proven successful in characterizing vegetation canopy structure and structural diversity for a range of traits, such as canopy height (Næsset & Økland, 2002), plant area index (PAI, Schneider et al., 2014), foliage height diversity (FHD, MacArthur & MacArthur, 1961), the vertical distribution of plant material in the canopy (either through PAI profiles (Marselis et al., 2018), or relative height (RH) of lidar energy (Drake et al., 2002; Dubayah et al., 2010)), and combinations thereof (Schneider et al., 2017). The study of structural diversity, in particular of forests, has gained increasing interest due to its importance for the carbon cycle, ecosystem services, plant and animal diversity, and habitat characterization (Bohn & Huth, 2017; Vierling et al., 2008; Davies & Asner, 2014).

How forests will react to ongoing global change is one of the main open questions in ecology and among the largest sources of uncertainty when predicting the carbon cycle and impacts of anthropogenic and climate change (Mitchard, 2018; Baccini et al., 2017; Hansen et al., 2019). At the same time, we are heading towards the sixth mass extinction of species on Earth (Ceballos et al., 2015; Barnosky et al., 2011) and suffering severe losses of biodiversity and key species (Isbell et al., 2017; Jones et al., 2018; Díaz et al., 2019), which calls for global biodiversity monitoring and immediate actions to be taken (Jetz et al., 2016). The Convention on Biological Diversity (CBD) helps guide those actions with a vision to ensure the valuation, conservation and restoration of biodiversity and its sustainable use through a set of policy-relevant targets (Mace et al., 2018). Many targets are not or only partially met though and the assessment of the state of biodiversity remains a challenge, as Díaz et al. (2019) point out summarizing the global assessment report of the Intergovernmental Platform on Biodiversity & Ecosystem Services (IPBES). Therefore, global mapping of structural diversity, as an important dimension of biodiversity and habitat quality, is of high importance and urgency (Jetz et al., 2016; Grassi et al., 2017).

The diversity of vegetation canopies influences light distribution and utilization within the canopy, with higher structural diversity often leading to a more effective use of energy and thus increased ecosystem productivity (Bohn & Huth, 2017; Williams et al., 2017). However, the lack of spatially explicit data at the landscape level and across biomes, climatic and edaphic gradients on plant structure, diversity and function limits our understanding of the diversity-productivity relationship (Schimel et al., 2015; Jetz et al., 2016; Sandel et al., 2015). Additionally to GEDI, operational and upcoming missions to measure ecosystem function (e.g. OCO-2/3, Ecostress, FLEX), structure (e.g. ICESat-2, MOLI, BIOMASS), and physiology (e.g. HISUI, EnMap, SBG) will help to fill these gaps by providing (near) global coverage and study related processes globally (Stavros et al., 2017). Structural diversity is one key aspect that could not only be linked directly to certain functions but also be incorporated in dynamic

vegetation models to improve predictions of carbon fluxes under global change drivers (Antonarakis et al., 2014; Rödig et al., 2018; Braghiere et al., 2019).

Increased structural diversity could provide a wider range of species niches and habitats supporting a larger number of species. Therefore, lidar-derived structural diversity can be a proxy for biodiversity of plants and animals (Vierling et al., 2008; Simonson et al., 2014). A range of ALS studies show good relationships between structural lidar measurements to plant species diversity (Hernández-Stefanoni et al., 2014; Zellweger et al., 2017), and Marselis et al. (2019) demonstrated the potential of GEDI to map tree species diversity in tropical forests. Lidar measurements can provide unique features to map and characterize habitats for animals, such as birds (Müller et al., 2010; Seavy et al., 2009), mammals (Zhao et al., 2012; Davies & Asner, 2014), and insects (Müller & Brandl, 2009; Müller et al., 2014), and to be used in species distribution models (Randin et al., 2020). GEDI is the first spaceborne sensor specifically designed to map 3D terrestrial vegetation structure, opening up a new era for biogeography and macroecology.

In this study, we simulate GEDI data (GEDI$_{sim}$) to assess its ability to capture diversity patterns from space. Advantages of a simulation study are that there are neither temporal nor geolocation mismatches between the reference airborne and the simulated spaceborne data and that a larger range of GEDI sampling densities can be simulated, including simulations with and without cloud cover. We investigate the following four research questions: (1) How do waveform-based structural traits of GEDI$_{sim}$ compare to discrete return ALS traits?, (2) Do trait to trait relationships hold between ALS and GEDI$_{sim}$?, (3) How does GEDI$_{sim}$ capture functional richness and beta diversity with and without the simulation of cloud cover?, and (4) What is the relationship between functional richness and beta diversity to the environment (climate, topography, soil)? We observe this over a heterogeneous mountain landscape, which provides a hot spot for plant biodiversity in the temperate and Mediterranean biomes comprising over 50% of California's plant diversity with more than 3500 native species (CWWR, 1996).

Materials and Methods

Study Area

The study area is located between Yosemite and Sequoia National Park (NP) in the southern Sierra Nevada mountains of California (Figure 1). The area spans 7380 km^2 of Kings Canyon NP and parts of Sequoia, Sierra and Inyo National Forests (NF). The area is characterized by complex mountainous terrain, spanning a total elevation range of 3000 m. The climate is Mediterranean with cool winters and long warm summers, with mean annual temperature ranging from -2.7 to 18.0°C (Bioclim, Fick & Hijmans, 2017). Summers are dry and prone to fires, with mean annual precipitation ranging from 125 to 1024 mm (Bioclim, Fick & Hijmans, 2017). Temperature and precipitation are highly variable and characterized by strong gradients from west to east due to the terrain and Pacific storm systems moving in from the west (CWWR, 1996).

The distribution of vegetation types is mainly driven by elevation and major valleys, but is variable locally depending on water availability, evaporative demand and disturbance history from fires, storm blowdowns, insect

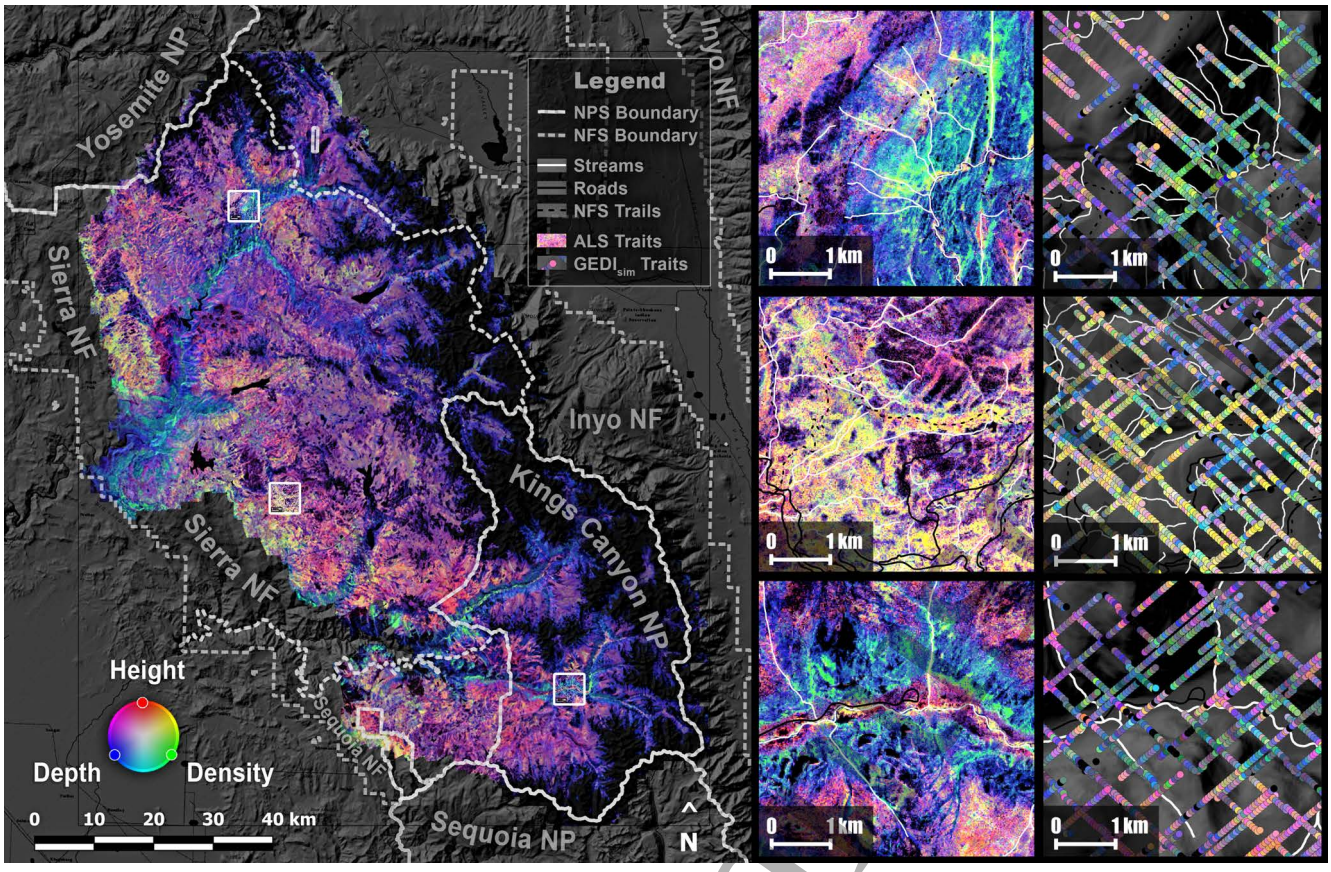

Figure 1: The study area spans 7380 km^2 of the Kings Canyon National Park (NP), Sequoia National Forest (NF), Sierra NF and Inyo NF in the southern Sierra Nevada mountains in California. The map shows a color composite of forest canopy height, density and depth, as the ratio of crown length to canopy height, at 20 m spatial resolution derived from airborne laser scanning of NASA's Airborne Snow Observatory. The right most panels show the corresponding GEDI traits simulated for two years. The background map is an SRTM DTM hillshade with ESRI's reference overlay. Solid and dashed white lines show NP and NF boundaries from the National Park Service (NPS) and National Forest Service (NFS). Right panels show close-ups of the map, NSF trails as black dashed lines, roads as black lines from www.mapcruzin.com and www.openstreetmap.org, and streams as white lines from the California Department of Fish and Wildlife (Christy, 2019).

and pathogen infestations, and avalanches (CWWR, 1996; Fites-Kaufman et al., 2007). The study area includes part of the lower elevation chaparral and oak savanna-type vegetation and some giant Sequoia trees in the south-western part. Dominant species are white and Douglas fir (*A. concolor, P. menziesii*), hemlocks (*T. mertensiana*), and lodgepole, sugar, ponderosa and Jeffrey pine (*P. contorta, P. lambertiana, P. ponderosa, P. jeffreyi*). Vegetation transitions to a zone of alpine vegetation at high elevations. Canyons are characterized by California laurel (*U. californica*), canyon live oak (*Q. chrysolepis*) and white alder, quaking aspen and tree willows (*A. rhombifolia, P. tremuloides, S. lasiolepis*) along streams and swampy meadows (CWWR, 1996; Fites-Kaufman et al., 2007).

Laser Scanning Data

Airborne laser scanning (ALS) data was acquired during summer of 2016 and 2017 as part of NASA's Airborne Snow Observatory (ASO). A full-waveform scanning lidar system (Riegl Q1560) was operated at an altitude of 6550 m asl, a nominal footprint size of 0.75 m to 1.5 m depending on elevation, and a swath width of ≈4.3 km. We combined multiple flight strips and optimized their co-registration and geolocation accuracy following Ferraz

et al. (2018) to create a dense point cloud with an average of 6 pts/m^2. A Delaunay triangulation was calculated from the points classified as ground to create the digital terrain model (DTM) and normalize the point cloud by the DTM. Additional details about the point cloud acquisition, processing and the data set itself will be published in Ferraz et al. (in preparation).

Spaceborne laser scanning data was simulated according to the expected GEDI sensor and acquisition characteristics using the approach of Hancock et al. (2019), which was previously tested (Marselis et al., 2019; Duncanson et al., 2020) and validated against NASA's airborne Land, Vegetation and Ice Sensor (LVIS) and related products (Hancock et al., 2019). We simulated two years of operational mission data assuming a 5% data transmission loss and 60% power allocation time, resulting in 395 days of data acquisition. This leads to 594,462 GEDI$_{sim}$ shots in total and 81 shots per square kilometer on average. However, GEDI's laser beam at 1064 nm does not penetrate clouds. Since cloud cover is highly clustered and mainly persistent at very high elevations, we used the cloud climatology data set by Wilson & Jetz (2016) to simulate the expected GEDI$_{sim}$ coverage. We randomly removed a percentage of days per month and 1 km^2 pixel from GEDI$_{sim}$ based on the average monthly 1 km^2 cloud frequency calculated based on the years 2000 to 2014 (Wilson & Jetz, 2016). This does not fully account for spatial clustering of clouds exceeding the 1 km^2 scale, which does not influence the diversity metrics derived at the same scale but might lead to more randomly distributed data gaps in the final maps. The final GEDI$_{sim}$ coverage over time simulated with cloud cover is shown in Suppl. Fig. S1.

Functional Trait Mapping

We used the approach of Schneider et al. (2014, 2017) to map canopy height, relative heights (RH) as percentiles of the vertical distribution of canopy points at 25, 50, 75 and 95%, plant area index (PAI) for the whole vertical column and per 10 m height layers (PAI0-10, PAI10-20, PAI20-30, PAI30-40) and foliage height diversity (FHD) from ASO ALS data. Additionally, we calculated the canopy ratio (CR) as the percentage of canopy depth to canopy height as follows:

$$CR = \frac{RH98 - RH25}{RH98}. \quad (1)$$

The above mentioned traits are also output of the GEDI simulator, and were used to test the potential of GEDI$_{sim}$. Relative height refers to the vertical distribution of returned lidar energy (mostly following the distribution of plant material), whereas plant area index defines plant area per unit ground area for a given vertical extent. An RH25 value of 6 m means that 25% of energy is located below 6 m from the ground, and a PAI0-10 of 2 means that there are 2 m^2 of leaves and branches per m^2 ground within 10 m from the ground. In both cases, the ground location has to be known. Here, we used GEDI$_{sim}$ traits derived using gaussian fitting to detect the ground. It has to be noted that for GEDI$_{sim}$ RH and FHD the full GEDI$_{sim}$ waveform was used as for the GEDI level 2 products. The traits were derived relative to the ground location but including ground energy due to the difficulty of separating ground and canopy energy with long pulses on slopes, whereas for the ALS RH metrics only canopy points above ground were used. We applied a correction factor to the GEDI$_{sim}$ RH values to limit the maximum height at very

steep slopes ($>\approx 50°$) for that reason (see Supplementary Figure S2 for more details). CR was then calculated using corrected GEDI$_{sim}$ RH as defined above (Eq. 1). Including ground energy in the case of GEDI$_{sim}$ also changes the interpretation of GEDI$_{sim}$ CR, since it is not only a function of vegetation height distribution but also fractional cover and the distribution of ground energy.

The GEDI$_{sim}$ metrics were calculated at the footprint level following the specifications of GEDI (Gaussian energy distribution within footprint with about 80% of the energy contained in a 22 m diameter). Therefore, we calculated the ALS area-based metrics on a 20 m grid to approximate a similar spatial grain.

Functional Diversity Mapping

We followed the concept of Schneider et al. (2017) to map plant functional diversity based on morphological canopy structure traits. Additionally to canopy height, density (PAI) and layering (FHD) which has been successfully mapped by Schneider et al. (2017) for a range of scales, we also included canopy ratio and the density of plant material from 0 to 10 m above ground. These are important descriptors of the canopy structure related to the compactness and filling of the canopy space as well as the presence of understory and low vegetation. To derive functional diversity, we analyzed the distribution of pixels or GEDI$_{sim}$ shots of an area of interest (e.g. 1 km^2) in the functional space defined by the five traits described above.

We adapted the concept of Schneider et al. (2017) to work with trait probability densities (TPD) in the functional trait space following Carmona et al. (2016b), allowing the derivation of functional richness (FRic) as the percentage of trait space occupied by a minimum density of pixels or GEDI$_{sim}$ shots (Fig. 2). In contrast to FRic derived as convex hull volume of pixels in trait space, this accounts for concave shapes or gaps in trait distributions. The approach works when dealing with varying sampling sizes per unit area, as is the case with the irregular spatial sampling of GEDI. Defining a density threshold for occupied space makes functional richness more robust and less susceptible to outliers than using the convex hull volume approach (Carmona et al., 2016a; Blonder, 2016). Moreover, the TPD approach provides a suitable concept to derive functional beta diversity (FBeta), defined as the non-overlapping areas of two density distributions from spatially separate areas (Carmona et al., 2016b, Fig. 2).

For the functional diversity calculations, we linearly scaled the traits from 0 to 1 with a 0.1% cut off of extreme values. We calculated TPD estimates on a 5D sampling grid of the trait space at 0.1 intervals for 1 km^2 spatial grid cells (mvksdensity in Matlab 2019a). We used the same grids for the calculation of ALS and GEDI$_{sim}$ trait densities. We then calculated functional richness as the percentage of number of trait space grid points with a TPD higher than 2 points per 0.1 kernel bandwidth. For functional beta diversity, we applied a moving window with a 3x3 neighborhood and calculated pair-wise functional beta diversity between each 1 km^2 pixel and its eight neighbors. Since strongest trait turnover takes place within the first few kilometers (Suppl. Fig. S5), we decided for the smallest window size of 3x3 km^2. We then calculated the average non-overlapping densities as functional beta diversity without applying a density threshold. Figure 2 illustrates the concept and sampling of the trait space for 1D, 2D, and 3D examples that can be extended to nD trait spaces.

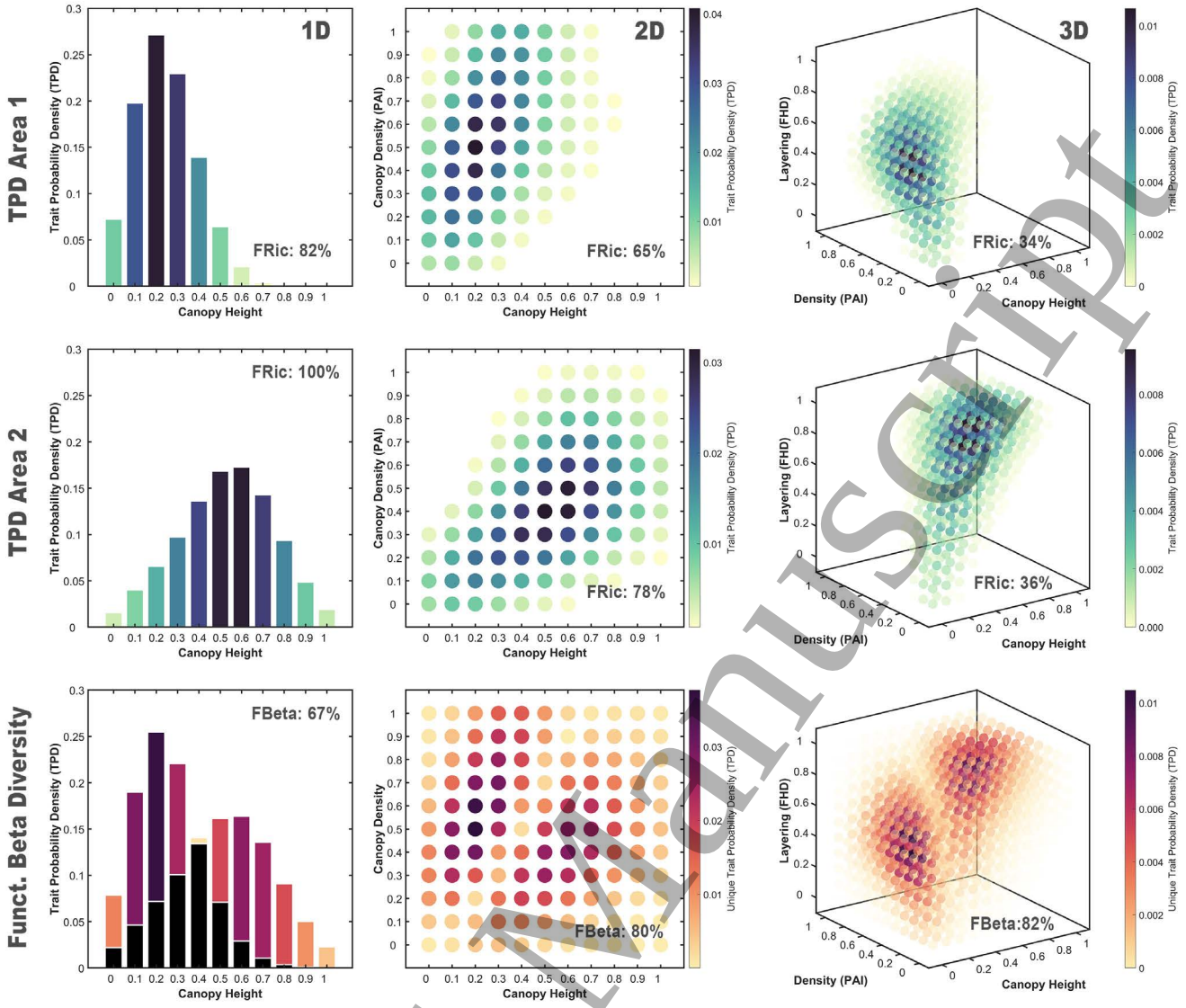

Figure 2: Trait probability density (TPD) in one, two and three dimensions (1D, 2D, 3D) based on canopy height, density as plant area index (PAI) and layering as foliage height diversity (FHD). This concept can by extended to any number of dimensions (nD) and allows to derive functional richness and functional beta diversity, among many other dimensions of functional diversity. We derived functional richness (FRic) as percentage of occupied trait space and functional beta diversity (FBeta) as percentage of unique, non-overlapping probability density. The example shows FRic for two adjacent 1 km^2 pixels (Area 1 & 2) and its corresponding FBeta.

Statistical Analyses

We compared GEDI$_{sim}$ and ALS traits by direct trait correlation using linear, power-law and logarithmic regression. We assess trait-to-trait relationships and compare traits in principal component space. We present the analysis for three components in the results based on Suppl. Fig. S6, with the third component still explaining 4.3 and 5.5% of the variance for ALS and GEDI$_{sim}$ traits (Suppl. Tab. S2). Since GEDI$_{sim}$ shots do not necessarily fall on ALS pixel centers, we calculated ALS traits at 10 m resolution and used bilinear interpolation to derive an ALS trait average at each GEDI$_{sim}$ shot location.

For interpretation of the functional diversity maps, we ran a random forest regression model to derive the most important environmental predictors of functional richness and beta diversity from a comprehensive set of climate, soil and topography variables from Fick & Hijmans (2017); Title & Bemmels (2018); Hengl et al. (2017); Conrad

et al. (2015), see Suppl. Tab. S3, S4 and S5. In a first step, we selected the top 15 predictors of functional richness for each set based on predictor importance estimates from permutations of out-of-bag predictor observations of 300 regression trees (fitrensemble, oobPermutedPredictorImportance in Matlab 2019a). We then applied a principal component analysis on the normalized predictors to map the major environmental patterns based on the first three components. We used the same 15 climate, soil and topography variables to estimate the importance on predicting beta diversity, and repeated the analysis using all 45 variables together.

Results

Functional Traits Comparison

The first step in evaluating GEDI's potential for mapping functional diversity is to compare GEDI$_{sim}$ traits to the ones derived from ALS data. On average, GEDI$_{sim}$ traits explained 68% of ALS trait variability for the 12 traits analyzed. Supplementary figure S3 shows the linear trait correlations with a tendency of higher GEDI$_{sim}$ values in steep areas of low vegetation height and density. The average r^2 increases to 0.72 in areas with less steep slopes $<10°$. Generally, estimates of the upper canopy are closer to ALS traits than from the mid- or understory, where GEDI$_{sim}$ RH values tend to be lower due to the inclusion of the ground energy. The most correlated traits are RH75, RH95 and maximum canopy height, as well as PAI in height layers of 10-20 m, 20-30 m, and 30-40 m with $r^2 \geq 0.80$. Most GEDI$_{sim}$ traits are linearly related to ALS traits, but CR and FHD show a stronger logarithmic and power-law relationship, respectively (see Suppl. Tab. S1).

Trait to Trait Relationships

Most plant functional traits show some degree of correlation with each other (Wright et al., 2004; Díaz et al., 2015). Those trait relationships can be important to characterize canopy structural types, as groups of plants with similar structural traits (Fahey et al., 2019; Huesca et al., 2019), but can also be indicators of stress, successional stage or disturbance (Dwyer & Laughlin, 2017; Lohbeck et al., 2012). Trait relationships generally hold between ALS and GEDI$_{sim}$ estimates, with GEDI$_{sim}$ capturing 59% of variation in ALS trait correlations (Fig. 3, see Suppl. Fig. S4 for the full matrix). GEDI$_{sim}$ traits include information from the canopy and the underlying terrain, and therefore show lower correlations among each other. Differences also arise from the differing trait distribution of PAI in the lowest layer 0 - 10 m above ground.

Major Trait Axes

We applied a principal component analysis to show major trait axes, possible correlations and trait contributions (loadings) to the first three components (Fig. 4). Small loadings could suggest little information content or redundancy with other traits, and thus guide trait selection. Height related traits mainly contributed to the first component, explaining 78% and 69% of total ALS and GEDI$_{sim}$ variance (see Suppl. Tab. S2). The contribution is

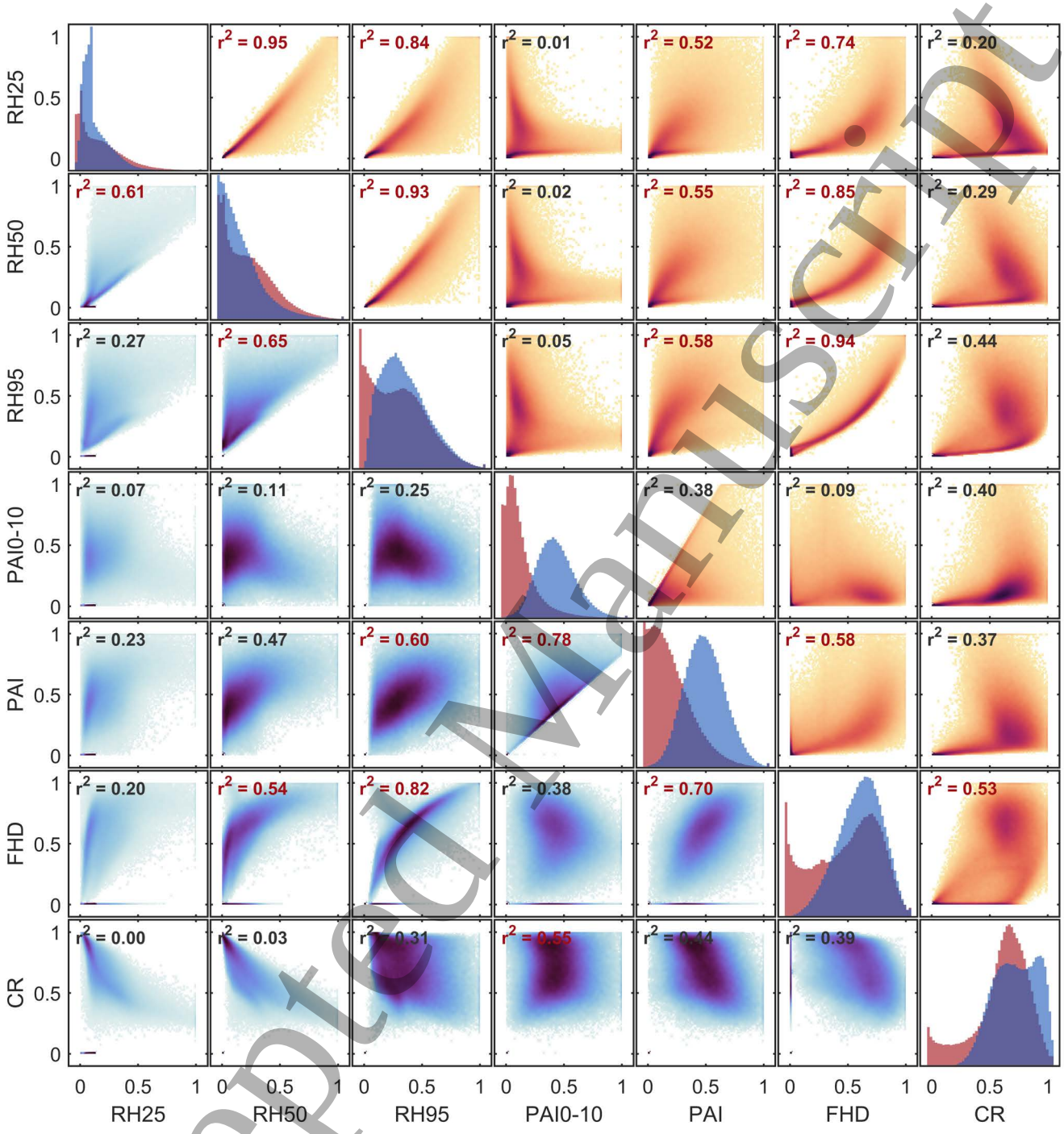

Figure 3: Correlation matrix of structural traits derived from airborne laser scanning (ALS) in the upper right half (yellow) and GEDI$_{sim}$ in the lower left half (blue). Note that patterns of the density scatter plots are mirrored due to the switch of trait axes. Darker color indicates higher density of points. Trait histograms are shown in the diagonal of the matrix. Trait relationships are generally well maintained between ALS and GEDI$_{sim}$, with strongest correlations among relative height values (RH) and lowest correlations of canopy ratio (CR) and plant area index (PAI) to other traits.

similar and none of the RH traits emerge as strong independent components, but the spread among the second and third component shows independent contributions to trait variability. FHD behaves similarly and is close to canopy height, but also shows a strong contribution to the first principal component on its own. Some of the strongest and most independent loadings stem from CR, PAI and density of the understory (PAI 0-10 m). These are strong contributors to the second and third components, explaining 13% and 4% of ALS and 18% and 6% of GEDI$_{sim}$ variance. Conversely, PAI layers above 10 m do not have a strong contribution, indicating little added information content due to many zero values and correlations to total PAI. This is the case for both ALS and GEDI$_{sim}$ derived traits.

GEDI's Ability to Map Functional Diversity from Space

We mapped functional richness and functional beta diversity from five structural traits, namely mean canopy height, plant area index, PAI at 0-10 m, foliage height diversity and canopy ratio, at 1 km^2 spatial resolution (Fig. 5). FRic is generally higher along the main valleys and in the western part of the study area, and lower in the central area and higher elevations. These patterns are related to temperature seasonality, soil organic carbon stock, cation exchange capacity and the generalized DTM, which are the best predictors of functional richness at the landscape scale based on a random forest regression model (Fig. 6). Soil organic carbon stock and variables controlling water availability through runoff (distance to river), radiation (sky view factor, diurnal anisotropic heating), and soil properties (occurrence of bedrock and distance to bedrock) are most important when combining all environmental variables in one model. These general patterns are well captured by GEDI$_{sim}$ too, both with and without the simulation of clouds (r^2 of 0.85, and r^2 of 0.75 with cloud cover). There is a slight underestimation of FRic in areas with denser, taller and more diverse forest canopies, whereas GEDI$_{sim}$ overestimates FRic in areas with lower vegetation and complex steep terrain (Suppl. Figs. S7, S9). Differences do not change much with cloud cover, but tend to be a bit more negatively biased due to the reduced number of samples (Suppl. Figs. S8, S10).

Functional beta diversity is an indicator of trait turnover and unique niche space that is not shared from one area to another (Carmona et al., 2016b). Therefore, Fbeta is high along the major valleys and canyons, where there is a strong shift in plant community traits between riparian and shrubby canyon vegetation to more open, mixed coniferous forests (Fig. 5). Moreover, FBeta is high at higher elevations, where vegetation gets patchy and its occurrence and structure are more strongly determined by geomorphological activity, avalanches, microtopography and soil. This is best described by changes in topography (ridge level, generalized DTM, sky view factor) followed by the occurrence of bedrock and changes in climatic moisture index (Fig. 6). GEDI$_{sim}$ captures some of these patterns, but with an overestimation when simulating clouds. The trait turnover along major valleys is less visible in GEDI$_{sim}$ derived maps, and the error is strongly related to sampling density (Suppl. Figs. S11, S12). The reduced number of GEDI$_{sim}$ shots when simulating cloud cover leads to a strong overestimation of beta diversity and a reduction of r^2 from 0.64 to 0.40 compared to ALS (Suppl. Fig. S8).

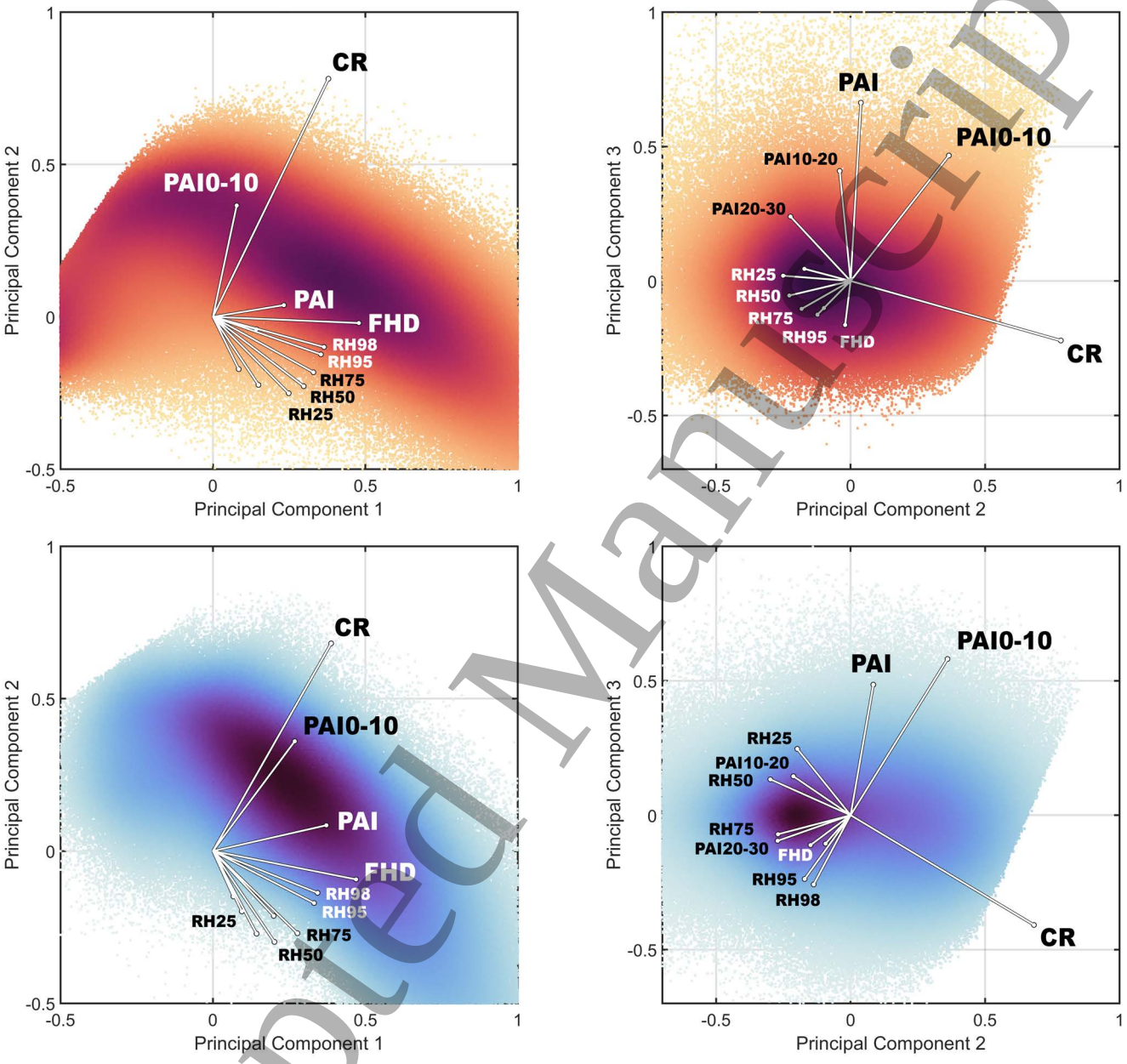

Figure 4: Principal component analysis of ALS (top row, orange) and GEDI$_{sim}$ (bottom row, blue) traits and their contributions to the first three components. The 12 structural traits are relative heights at 25-99% percentiles (RH25-RH99), foliage height diversity (FHD), plant area index (PAI), PAI at 10 m height intervals (PAI0-10 to PAI30-40) and canopy ratio (CR). The length of the lines corresponds to the loadings or strength of contribution of the traits to the principal components. Traits with small loadings are not labeled.

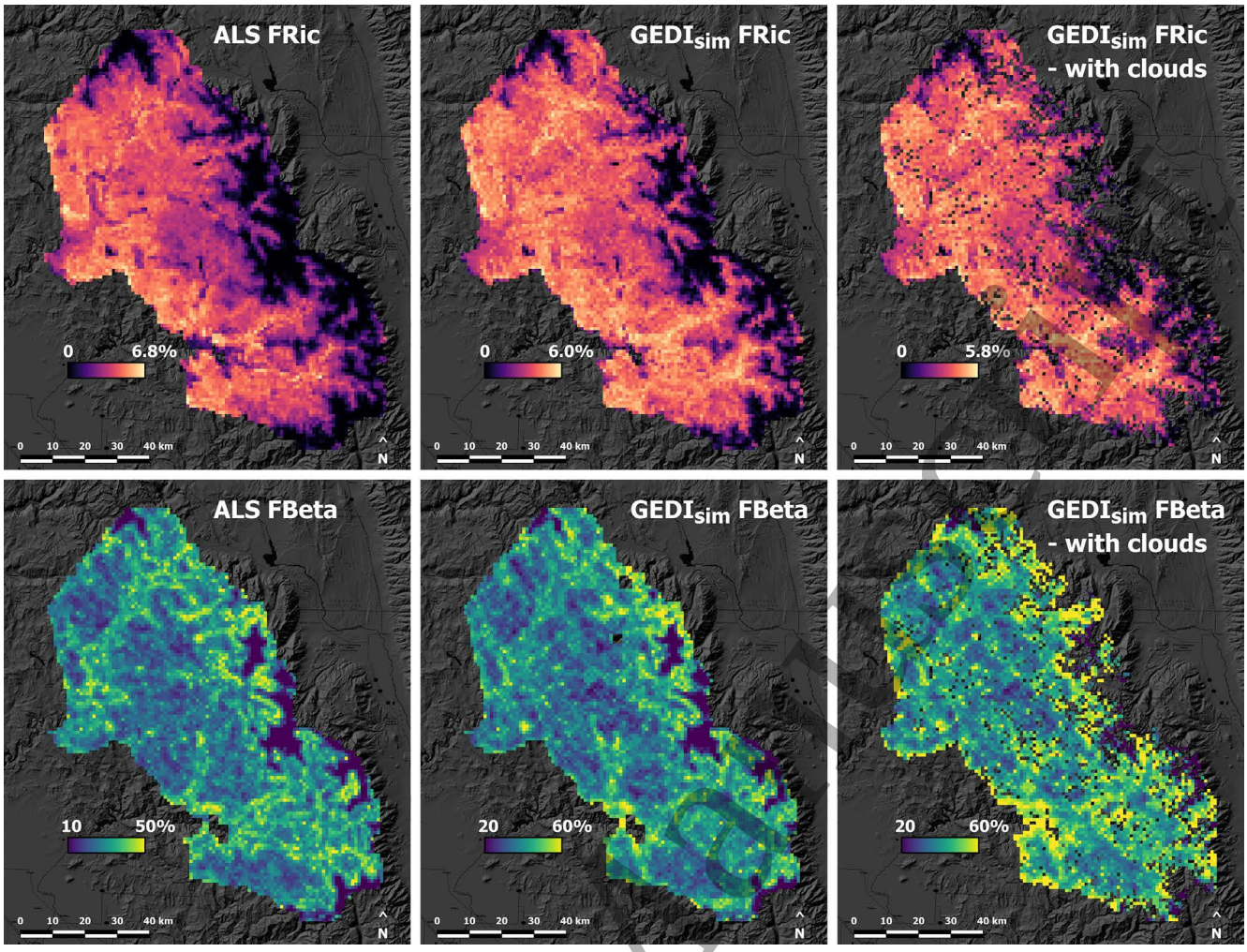

Figure 5: Functional richness (top row) and functional beta diversity (bottom row) at 1 km resolution in percent of filled and non-overlapping trait probability density space, respectively. Maps on the left are derived from spatially continuous airborne laser scanning (ALS) traits, compared to maps derived from simulated GEDI data (GEDI$_sim$) without (middle) and with cloud cover (right).

Discussion

GEDI is designed to provide 3D canopy structure information from space by sampling vertical canopy profiles with a 25 m footprint laser. The measured laser waveform includes the energy returned from the ground, which can be strongly elongated in steep terrain. Ground energy might be mixed with energy returned from understory vegetation or small trees. In this case, disentangling the contribution from ground and vegetation canopy is challenging and can lead to inaccurate estimates of canopy structure traits (Ilangakoon et al., in review), such as the systematic overestimation of high canopy ratio and low foliage height diversity. In extreme cases, complex steep terrain with boulders can look like vegetation due to multi-modal ground returns (Hancock et al., 2012). Considering the challenging terrain, GEDI$_{sim}$ performed well in terms of structural trait retrieval with best results in flat areas and for traits related to the upper canopy. Further research is needed to develop an algorithm to decompose the waveform into ground and canopy energy, but issues might remain in steep areas with dense understory vegetation.

Functional diversity estimates are dependent on the accuracy and selection of traits and the spatial scale used

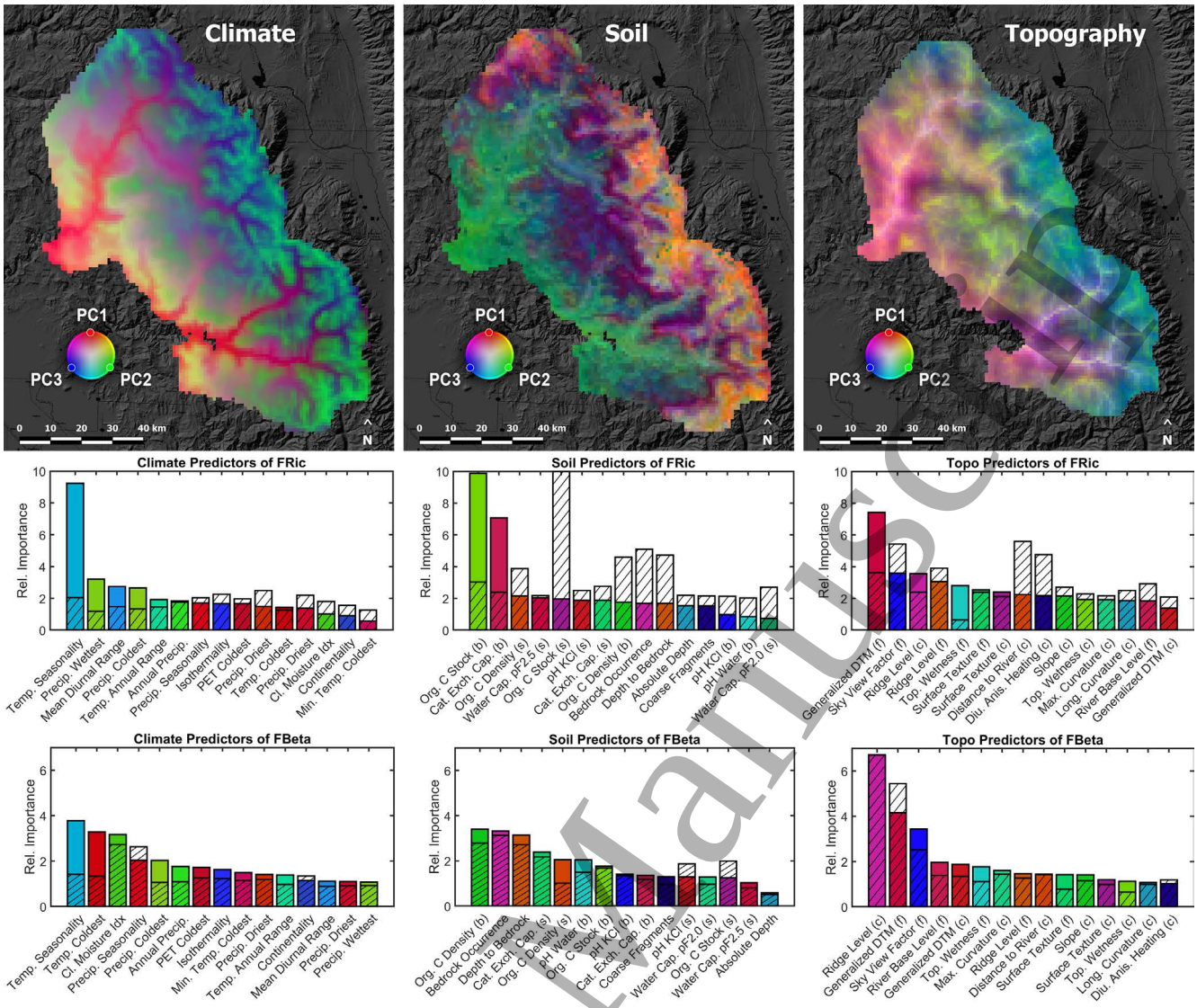

Figure 6: Environmental variables grouped by climate, soil and topography, and their importance to predict functional richness (FRic) and functional beta diversity (FBeta). The maps illustrate the major axes of variation, being colored by the first three principal components of the 15 best predictors of FRic. The panels below the maps show relative importance of the variables to predict FRic (middle) and FBeta (bottom) for each group of variables. The colors correspond to their contribution to the first three components as shown on the maps. The dashed bars show the relative importance when all 45 variables are used in one model.

to derive them (Funk et al., 2017; Anderson, 2018). For functional diversity analyses, we suggest to include plant functional traits that are functionally relevant in terms of growth, reproduction or survival (Violle et al., 2007; Díaz et al., 2015), ecologically relevant in terms of competition, niche space or succession (Kunstler et al., 2016; Cadotte, 2017), and that build independent trait axes without functional redundancy or over-representation of one trait axis (Petchey & Gaston, 2006). We followed this suggestion and the principal component analysis showing five major trait axes for both ALS and GEDI$_{sim}$ traits. Optimizing the trait selection towards best correlation to ALS could have potentially improved GEDI$_{sim}$ results, but also changed the meaning and relevance of functional diversity. The impact of changing trait combinations and number of traits on diversity estimates is not assessed here, but can be relevant depending on the science question, application and scale (Roscher et al., 2012; Zhu et al., 2017; Jarzyna & Jetz, 2018). Trait selection might be less critical at large scales where traits and their

spatial organization are more likely to be correlated, as was shown by Schneider et al. (2017) for diversity of morphological and physiological forest traits along an environmental gradient.

We mapped functional diversity at 1 km resolution, which we think is the smallest reasonable resolution for our application with 72% of pixels having more than 20 and 44% more than 40 GEDI$_{sim}$ shots per pixel (see Suppl. Fig. S15). This number drops to only 12% and 0% respectively at 500 m resolution considering simulated cloud cover. The results also show that a lower resolution might be needed to create a gap-free diversity product of the area. The fusion with additional spatially continuous data sets like Sentinel, Landsat, Planet, or the upcoming NISAR might help to create a higher resolution gridded product. Nevertheless, the GEDI$_{sim}$ data analysis in this study indicate that GEDI will provide a unique spatial grain and extent on canopy structure and diversity, which has previously been unavailable and could help scale existing ground based trait and diversity maps. For example, the global trait maps of Bruelheide et al. (2018) are interpolated at 10 km with many remaining gaps, whereas Butler et al. (2017) modeled a continuous global coverage but for 50 km cells. Current global data sets of animal diversity are produced at 2° (≈200 km) by Hurlbert & Jetz (2007); Pollock et al. (2017). Functional richness calculated as the filled probability density space of five major canopy structure traits shows broad patterns of diversity cold and hot spots. The availability of water is strongly associated with those patterns in a Mediterranean climate with prolonged summmer dryness. Therefore, environmental variables related to soil water availability, evaporative demand and incident radiation, as well as distance to stream and precipitation are shaping the distribution of plant communities. These might be the main drivers of structural diversity, whereas the strong link of soil organic carbon stock and density with plant functional richness could be a result of the higher plant productivity and biomass in more diverse ecosystems. Many studies have shown positive effects of plant biodiversity on productivity (Liang et al., 2016; Huang et al., 2018), with a strong link through structural diversity as a regulator for radiation interception and increased resource use efficiency (Bohn & Huth, 2017; Williams et al., 2017). Those general patterns of functional richness agree with total species richness reported by Wathen et al. (2014) for the Kings Canyon NP, and are captured well both by GEDI$_{sim}$ simulated with and without clouds.

Abiotic factors are shaping the distribution of plant structure and species, especially in a water and temperature limited system as presented here. However, the importance of individual variables has to be taken with care, since random forest feature importance can strongly vary depending on how many co-varying features were included in the analysis. Furthermore, the SoilGrids dataset was modeled with spatial covariates including long-term MODIS enhanced vegetation index, near and middle infrared reflectance and land surface temperature, among others (Hengl et al., 2017). Therefore, correlations to functional diversity might not purely reflect soil properties.

Overestimation of functional richness happens in areas with low vegetation or sparse coverage and complex, steep terrain due to topography effects on the laser waveform discussed above. Underestimation occurs in areas of higher canopy structural complexity and tree height due to the spatial sampling of GEDI. Since functional richness is a measure of total occupied niche space, the spatial sampling and heterogeneity of the landscape will determine how much of the total trait diversity GEDI can capture. When sampling density decreases with increasing cloud cover, it is more likely to miss certain trait combinations and thus underestimate functional richness. This could

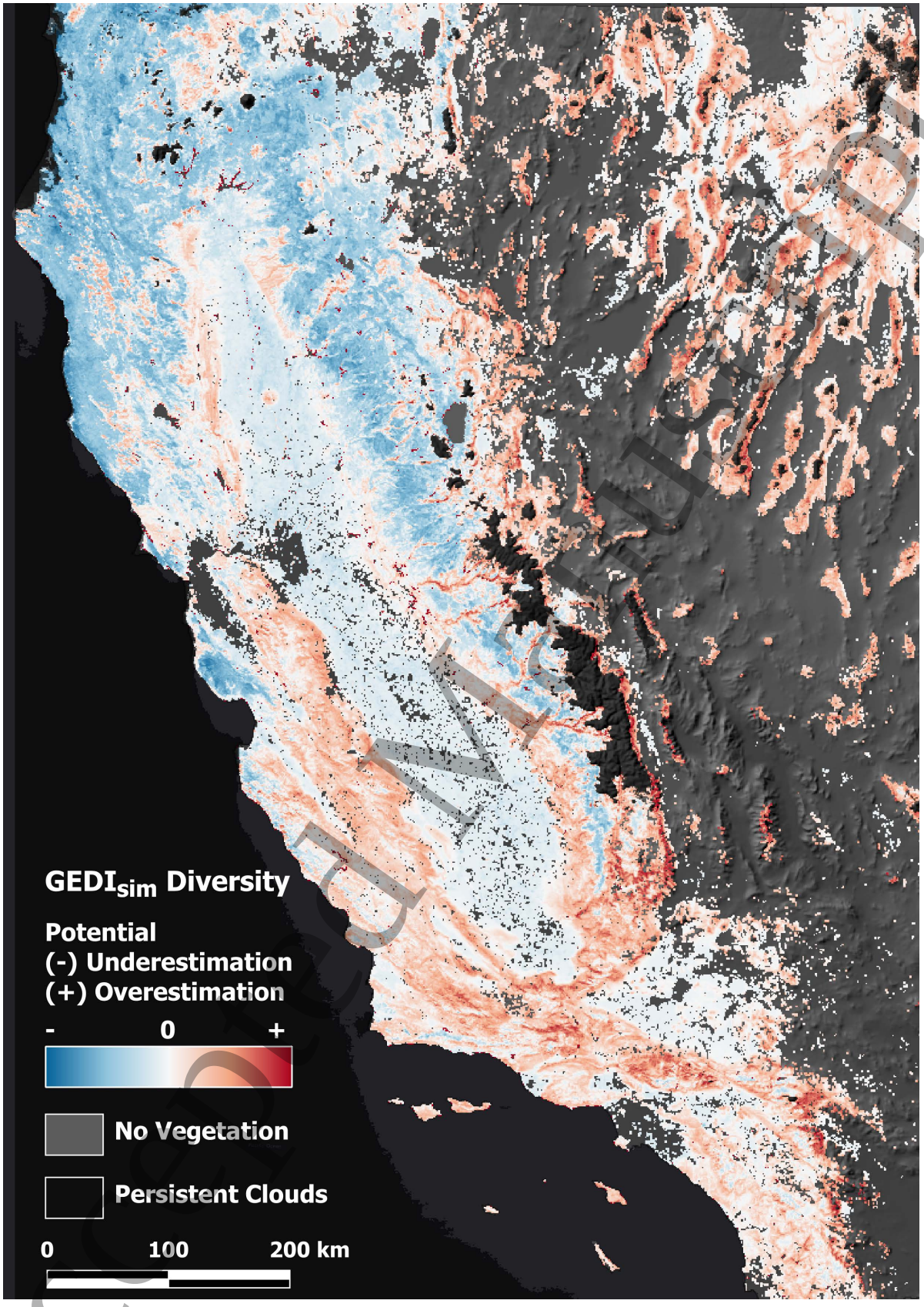

Figure 7: Prediction of possible over- and underestimation of GEDI diversity over California using a stepwise linear regression model with terrain slope, topographic diversity, tree cover, cloud frequency and interaction terms. Areas with no vegetation were masked when their greenest pixel of a year had an NDVI below 0.1.

have implications for mapping tropical forests, which are especially effected by cloud cover but would require a dense sampling to capture the large heterogeneity of canopy structure. At our study site, a simple relationship between terrain slope, topographic diversity and tree cover can explain about a third of the observed over- and underestimation of functional richness (Suppl. Fig. S13 and S14), and could provide a guide to build hypotheses on where to expect potential over- and underestimation of diversity in California (Fig. 7). One caveat of the current approach is that we are not providing a ground validation, which is challenging and also potentially inaccurate at 20 m grain and 1 km extent. Therefore, we rely on comparisons to state-of-the-art ALS with wall-to-wall coverage. Future research will be needed to further test this method at additional study sites, covering a larger range of vegetation types and environments, and with real GEDI data.

Functional beta diversity is more complex, since it describes trait turnover and shifts in trait distributions from one region to another. At the scale of 1 km and 3x3 km neighborhoods, it is more related to trait turnover among large environmental gradients than local species beta diversity between communities. The beta diversity patterns shown in Fig. 5 are clearly reflecting the shifts in canopy structure between wetter and more densely vegetated valleys and canyons and drier open areas with sparser coniferous forests, best reflected by change in topographic variables. This is in line with Jucker et al. (2018), who found that topography is shaping the distribution of forest structure and diversity through its impact on microclimate and local soil variability, which might not be captured by the more broadly modeled global climate and soil data sets. Moreover, it shows the patchiness of vegetation at higher elevation, where canopy structure can change dramatically based on disturbance history. These patterns are captured by GEDI$_{sim}$ simulated without clouds, but disappear with decreasing sampling density. There is no clear threshold, but the errors seem to stabilize at around 40 or more samples per unit area in this study area (Suppl. Fig. S11 and S12), and potentially more in regions of higher local variability. Fusion with other structural data sets, e.g. from ICESat-2, might overcome issues due to low sampling density and may enable improved capabilities (Neuenschwander & Pitts, 2019).

The implication of near-global maps of functional richness and beta diversity for assessing the state of biodiversity, as mandated by IPBES, and related CBD targets could be large, because it's breaking the ground for new ways of observing ecosystem structure that have not been available before. Ecosystem structure has been identified as a key Essential Biodiversity Variable (EBV) class (Skidmore et al., 2015), and the proposed approach could contribute or be added to candidate EBVs as well as CBD targets 5 (Habitat loss, fragmentation and degradation), 7 (Sustainable management) and 15 (carbon sequestration, ecosystem resilience), see O'Connor et al. (2015). In combination with models or other sources of biodiversity data, the mapping of functional richness and beta diversity with GEDI could also help address CBD targets 9 (Control of invasive alien species), 11 (protected areas) and 14 (ecosystem services safeguarded), and more broadly help to sustainably manage forests and monitor land degradation and biodiversity loss (Sustainable Development Goal 15, Díaz et al., 2019). GEDI enables a whole suite of new ecosystem structure products that can be used for monitoring in the future (Dubayah et al., 2020). Finally, for a long time the diversity of plant canopy structure was neglected or oversimplified in global Earth system models, leading to potential errors in the radiation budget and underestimation of plant photosynthesis

(Braghiere et al., 2019). This could be changed with the availability of a GEDI diversity product and its integration into dynamic vegetation models (Schimel et al., 2019).

Conclusion

GEDI provides unique measurements of 3D canopy structure from space, and the simulation study presented here shows the potential to successfully characterize functional richness at large spatial scales. Care has to be taken in steep areas with low or sparse vegetation cover to not mistakenly treat variation in ground returns as plant functional richness. Implications for the understanding of large-scale patterns of plant canopy structure, structural diversity and potential links to animal diversity, movement and habitats are immense, and could be transformative for global ecology (Schimel et al., 2019). Our results suggest that functional richness could be estimated from GEDI data with little influence by sampling density, whereas functional beta diversity shows large uncertainty in areas of low coverage. Estimating biodiversity from functional traits could have a range of advantages. GEDI provides consistent measurements of canopy height, layering and density over all of the world's temperate, Mediterranean and tropical forests, except for the discussed issues in mountainous areas and possible data gaps due to cloud cover. This provides a new view on biodiversity, including intra-specific diversity and the vertical component of canopy structure in a range of natural, managed and disturbed forests. This could help monitor biodiversity and policy targets, and greatly improve the representation of plant canopies in dynamic vegetation and land surface models, improving our understanding of the carbon cycle and ecological forecasting.

GEDI products are being released month by month on NASA's LP DAAC since January 2020. Dubayah et al. (2020) show the excellent fidelity of GEDI on-orbit waveforms compared to airborne lidar, but future research is needed to test GEDI level 2 A and B products for functional diversity mapping across biomes, once sufficient coverage is available at near-global extent.

Acknowledgements

The research carried out at the Jet Propulsion Laboratory, California Institute of Technology, was under a contract with the National Aeronautics and Space Administration (80NM0018D0004). Government sponsorship is acknowledged. Funding for RD and SH was provided by NASA contract #NNL 15AA03C to the University of Maryland for the development and execution of the GEDI mission. We thank Marcos Longo, Gary Geller and Ewa Czyż for fruitful discussions on topics related to the manuscript. We thank Kat J. Bormann and Tom H. Painter from the JPL Airborne Snow Observatory for the airborne laser scanning data. Funding and support for the Airborne Snow Observatory surveys was provided by NASA, the California Department of Water Resources, JPL investments, and the Kings Basin Water Authority.

The authors declare no conflict of interest.

Data Availability

The data that support the findings of this study are available upon reasonable request from the authors, and will be openly available at the NASA Distributed Active Archive Center (DAAC) at NSIDC and published in Ferraz et al. (in preparation) at a later stage.

References

Anderson, C. B. (2018). Biodiversity monitoring, earth observations and the ecology of scale. *Ecology Letters*, *21*, 1572–1585.

Antonarakis, A. S., Munger, J. W., & Moorcroft, P. R. (2014). Imaging spectroscopy- and lidar-derived estimates of canopy composition and structure to improve predictions of forest carbon fluxes and ecosystem dynamics. *Geophysical Research Letters*, *41*, 2535–2542.

Baccini, A., Walker, W., Carvalho, L., Farina, M., Sulla-Menashe, D., & Houghton, R. A. (2017). Tropical forests are a net carbon source based on aboveground measurements of gain and loss. *Science*, *358*, 230–234.

Barnosky, A. D., Matzke, N., Tomiya, S., Wogan, G. O., Swartz, B., Quental, T. B., Marshall, C., McGuire, J. L., Lindsey, E. L., Maguire, K. C., Mersey, B., & Ferrer, E. A. (2011). Has the Earth's sixth mass extinction already arrived? *Nature*, *471*, 51–57.

Blonder, B. (2016). Pushing Past Boundaries for Trait Hypervolumes: A Response to Carmona et al. *Trends in Ecology & Evolution*, *31*, 665–667.

Bohn, F. J., & Huth, A. (2017). The importance of forest structure to biodiversity–productivity relationships. *Royal Society Open Science*, *4*, 160521.

Braghiere, R. K., Quaife, T., Black, E., He, L., & Chen, J. M. (2019). Underestimation of Global Photosynthesis in Earth System Models Due to Representation of Vegetation Structure. *Global Biogeochemical Cycles*, (p. 2018GB006135).

Bruelheide, H., Dengler, J., Purschke, O., Lenoir, J., Jiménez-Alfaro, B., Hennekens, S. M., Botta-Dukát, Z., Chytrý, M., Field, R., Jansen, F., Kattge, J., Pillar, V. D., Schrodt, F., Mahecha, M. D., Peet, R. K., Sandel, B., van Bodegom, P., Altman, J., Alvarez-Dávila, E., Arfin Khan, M. A. S., Attorre, F., Aubin, I., Baraloto, C., Barroso, J. G., Bauters, M., Bergmeier, E., Biurrun, I., Bjorkman, A. D., Blonder, B., Čarni, A., Cayuela, L., Černý, T., Cornelissen, J. H. C., Craven, D., Dainese, M., Derroire, G., De Sanctis, M., Díaz, S., Doležal, J., Farfan-Rios, W., Feldpausch, T. R., Fenton, N. J., Garnier, E., Guerin, G. R., Gutiérrez, A. G., Haider, S., Hattab, T., Henry, G., Hérault, B., Higuchi, P., Hölzel, N., Homeier, J., Jentsch, A., Jürgens, N., Kącki, Z., Karger, D. N., Kessler, M., Kleyer, M., Knollová, I., Korolyuk, A. Y., Kühn, I., Laughlin, D. C., Lens, F., Loos, J., Louault, F., Lyubenova, M. I., Malhi, Y., Marcenò, C., Mencuccini, M., Müller, J. V., Munzinger, J., Myers-Smith, I. H., Neill, D. A., Niinemets, Ü., Orwin, K. H., Ozinga, W. A., Penuelas, J., Pérez-Haase, A., Petřík, P., Phillips, O. L., Pärtel, M., Reich, P. B., Römermann, C., Rodrigues, A. V., Sabatini, F. M., Sardans, J., Schmidt, M., Seidler, G., Silva Espejo, J. E., Silveira, M., Smyth, A., Sporbert, M., Svenning, J.-C., Tang, Z., Thomas, R., Tsiripidis, I., Vassilev, K., Violle, C., Virtanen, R. et al. (2018). Global trait–environment relationships of plant communities. *Nature Ecology & Evolution*, *2*, 1906–1917.

Butler, E. E., Datta, A., Flores-Moreno, H., Chen, M., Wythers, K. R., Fazayeli, F., Banerjee, A., Atkin, O. K., Kattge, J., Amiaud, B., Blonder, B., Boenisch, G., Bond-Lamberty, B., Brown, K. A., Byun, C., Campetella, G., Cerabolini, B. E. L., Cornelissen, J. H. C., Craine, J. M., Craven, D., de Vries, F. T., Díaz, S., Domingues, T. F., Forey, E., González-Melo, A., Gross, N., Han, W., Hattingh, W. N., Hickler, T., Jansen, S., Kramer, K., Kraft, N. J. B., Kurokawa, H., Laughlin, D. C., Meir, P., Minden, V., Niinemets, Ü., Onoda, Y., Peñuelas, J., Read, Q., Sack, L., Schamp, B., Soudzilovskaia, N. A., Spasojevic, M. J., Sosinski, E., Thornton, P. E., Valladares, F., van Bodegom, P. M., Williams, M., Wirth, C., & Reich, P. B. (2017). Mapping local and global variability in plant trait distributions. *Proceedings of the National Academy of Sciences*, (p. 201708984).

Cadotte, M. W. (2017). Functional traits explain ecosystem function through opposing mechanisms. *Ecology Letters*, (pp. 1–8).

Carmona, C. P., de Bello, F., Mason, N. W., & Lepš, J. (2016a). The Density Awakens: A Reply to Blonder. *Trends in Ecology & Evolution*, *31*, 667–669.

Carmona, C. P., de Bello, F., Mason, N. W., & Lepš, J. (2016b). Traits Without Borders: Integrating Functional Diversity Across Scales. *Trends in Ecology & Evolution*, *31*, 382–394.

Ceballos, G., Ehrlich, P. R., Barnosky, A. D., García, A., Pringle, R. M., & Palmer, T. M. (2015). Accelerated modern human–induced species losses: Entering the sixth mass extinction. *Science Advances*, *1*, e1400253.

Christy, T. (2019). California Streams. Calif. Dept. of Fish and Wildlife. Biogeographic Information and Observation System (BIOS). Retrieved May 27, 2020. URL: `https://data.cnra.ca.gov/dataset/california-streams`.

Conrad, O., Bechtel, B., Bock, M., Dietrich, H., Fischer, E., Gerlitz, L., Wehberg, J., Wichmann, V., & Böhner, J. (2015). System for Automated Geoscientific Analyses (SAGA) v. 2.1.4. *Geoscientific Model Development*, *8*, 1991–2007.

CWWR (1996). Sierra Nevada Ecosystems. In *Status of the Sierra Nevada, Sierra Nevada Ecosystem Project, Final Report to Congress*. Centers for Water and Wildland Resources, University of California Davis.

Davies, A. B., & Asner, G. P. (2014). Advances in animal ecology from 3D-LiDAR ecosystem mapping. *Trends in Ecology and Evolution*, *29*, 681–691.

Díaz, S., Kattge, J., Cornelissen, J. H. C., Wright, I. J., Lavorel, S., Dray, S., Reu, B., Kleyer, M., Wirth, C., Prentice, I. C., Garnier, E., Bönisch, G., Westoby, M., Poorter, H., Reich, P. B., Moles, A. T., Dickie, J., Gillison, A. N., Zanne, A. E., Chave, J., Wright, S. J., Sheremet'ev, S. N., Jactel, H., Christopher, B., Cerabolini, B., Pierce, S., Shipley, B., Kirkup, D., Casanoves, F., Joswig, J. S., Günther, A., Falczuk, V., Rüger, N., Mahecha, M. D., & Gorné, L. D. (2015). The global spectrum of plant form and function. *Nature*, *529*, 1–17.

Díaz, S., Settele, J., Brondizio, E. S., Ngo, H. T., Agard, J., Arneth, A., Balvanera, P., Brauman, K. A., Butchart, S. H. M., Chan, K. M. A., Garibaldi, L. A., Ichii, K., Liu, J., Subramanian, S. M., Midgley, G. F., Miloslavich, P., Molnár, Z., Obura, D. O., Pfaff, A., Polasky, S., Purvis, A., Razzaque, J., Reyers, B., Chowdhury, R. R., Shin, Y.-J., Visseren-Hamakers, I., Willis, K., & Zayas, C. N. (2019). Pervasive human-driven decline of life on Earth points to the need for transformative change. *Science*, *1327*.

Drake, J. B., Dubayah, R. O., Clark, D. B., Knox, R. G., Blair, J. B., Hofton, M. A., Chazdon, R. L., Weishampel, J. F., & Prince, S. (2002). Estimation of tropical forest structural characteristics, using large-footprint lidar. *Remote Sensing of Environment*, *79*, 305–319.

Dubayah, R., Blair, J. B., Goetz, S., Fatoyinbo, L., Hansen, M., Healey, S., Hofton, M., Hurtt, G., Kellner, J., Luthcke, S., Armston, J., Tang, H., Duncanson, L., Hancock, S., Jantz, P., Marselis, S., Patterson, P., Qi, W., & Silva, C. (2020). The Global Ecosystem Dynamics Investigation: High-resolution laser ranging of the Earth's forests and topography. *Science of Remote Sensing*, (p. 100002).

Dubayah, R. O., Sheldon, S. L., Clark, D. B., Hofton, M. A., Blair, J. B., Hurtt, G. C., & Chazdon, R. L. (2010). Estimation of tropical forest height and biomass dynamics using lidar remote sensing at la Selva, Costa Rica. *Journal of Geophysical Research: Biogeosciences*, *115*, 1–17.

Duncanson, L., Neuenschwander, A., Hancock, S., Thomas, N., Fatoyinbo, T., Simard, M., Silva, C. A., Armston, J., Luthcke, S. B., Hofton, M., Kellner, J. R., & Dubayah, R. (2020). Biomass estimation from simulated GEDI, ICESat-2 and NISAR across environmental gradients in Sonoma County, California. *Remote Sensing of Environment*, *242*, 111779.

Dwyer, J. M., & Laughlin, D. C. (2017). Constraints on trait combinations explain climatic drivers of biodiversity: the importance of trait covariance in community assembly. *Ecology Letters*, *20*, 872–882.

Fahey, R., Atkins, J., Gough, C., Hardiman, B., Nave, L., Curtis, P., Tallant, J., Turner, L., Nadehoffer, K., Vogel, C., Scheuermann, C., Stuart-Haentjens, E., Fotis, A., & Ricart., R. (2019). Defining a spectrum of integrative trait-based vegetation canopy structural types. *Ecological Applications*, .

Ferraz, A., Saatchi, S., Bormann, K., & Painter, T. (2018). Fusion of NASA Airborne Snow Observatory (ASO) Lidar Time Series over Mountain Forest Landscapes. *Remote Sensing*, *10*, 164.

Ferraz, A., Schneider, F. D., Painter, T. H., Bormann, K. J., Hancock, S., & Schimel, D. S. (). From lidar waveforms to vegetation products: 7380 km2 of high-resolution airborne and simulated GEDI data over the Sierra Nevada, California. *Nature Scientific Data*, (p. in prep).

Fick, S. E., & Hijmans, R. J. (2017). WorldClim 2: new 1-km spatial resolution climate surfaces for global land areas. *International Journal of Climatology*, *37*, 4302–4315.

Fites-Kaufman, J. A., Rundel, P. W., Stephenson, N., & Weixelman, D. A. (2007). *Montane and subalpine vegetation of the Sierra Nevada and Cascade ranges*. December 2013.

Funk, J. L., Larson, J. E., Ames, G. M., Butterfield, B. J., Cavender-Bares, J., Firn, J., Laughlin, D. C., Sutton-Grier, A. E., Williams, L., & Wright, J. (2017). Revisiting the Holy Grail: using plant functional traits to understand ecological processes. *Biological Reviews*, *92*, 1156–1173.

Grassi, G., House, J., Dentener, F., Federici, S., Den Elzen, M., & Penman, J. (2017). The key role of forests in meeting climate targets requires science for credible mitigation. *Nature Climate Change*, *7*, 220–226.

Hancock, S., Hofton, M., Sun, X., Tang, H., Kellner, J. R., Armston, J., Duncanson, L. I., & Dubayah, R. (2019). The GEDI simulator: A large-footprint waveform lidar simulator for calibration and validation of spaceborne missions. *Earth and Space Science*, (pp. 1–17).

Hancock, S., Lewis, P., Foster, M., Disney, M., & Muller, J.-P. (2012). Measuring forests with dual wavelength lidar: A simulation study over topography. *Agricultural and Forest Meteorology*, *161*, 123–133.

Hansen, M. C., Potapov, P., & Tyukavina, A. (2019). Comment on "Tropical forests are a net carbon source based on aboveground measurements of gain and loss". *Science*, *363*, eaar3629.

Hengl, T., Mendes de Jesus, J., Heuvelink, G. B. M., Ruiperez Gonzalez, M., Kilibarda, M., Blagotić, A., Shangguan, W., Wright, M. N., Geng, X., Bauer-Marschallinger, B., Guevara, M. A., Vargas, R., MacMillan, R. A., Batjes, N. H., Leenaars, J. G. B., Ribeiro, E., Wheeler, I., Mantel, S., & Kempen, B. (2017). SoilGrids250m: Global gridded soil information based on machine learning. *PLOS ONE*, *12*, e0169748.

Hernández-Stefanoni, J. L., Dupuy, J. M., Johnson, K. D., Birdsey, R., Tun-Dzul, F., Peduzzi, A., Caamal-Sosa, J. P., Sánchez-Santos, G., & López-Merlín, D. (2014). Improving species diversity and biomass estimates of tropical dry forests using airborne LiDAR. *Remote Sensing*, *6*, 4741–4763.

Huang, Y., Chen, Y., Castro-Izaguirre, N., Baruffol, M., Brezzi, M., Lang, A., Li, Y., Härdtle, W., von Oheimb, G., Yang, X., Liu, X., Pei, K., Both, S., Yang, B., Eichenberg, D., Assmann, T., Bauhus, J., Behrens, T., Buscot, F., Chen, X.-Y., Chesters, D., Ding, B.-Y., Durka, W., Erfmeier, A., Fang, J., Fischer, M., Guo, L.-D., Guo, D., Gutknecht, J. L. M., He, J.-S., He, C.-L., Hector, A., Hönig, L., Hu, R.-Y., Klein, A.-M., Kühn, P., Liang, Y., Li, S., Michalski, S., Scherer-Lorenzen, M., Schmidt, K., Scholten, T., Schuldt, A., Shi, X., Tan, M.-Z., Tang, Z., Trogisch, S., Wang, Z., Welk, E., Wirth, C., Wubet, T., Xiang, W., Yu, M., Yu, X.-D., Zhang, J., Zhang, S., Zhang, N., Zhou, H.-Z., Zhu, C.-D., Zhu, L., Bruelheide, H., Ma, K., Niklaus, P. A., & Schmid, B. (2018). Impacts of species richness on productivity in a large-scale subtropical forest experiment. *Science*, *362*, 80–83.

Huesca, M., Roth, K. L., García, M., & Ustin, S. L. (2019). Discrimination of Canopy Structural Types in the Sierra Nevada Mountains in Central California. *Remote Sensing*, *11*, 1100.

Hurlbert, A. H., & Jetz, W. (2007). Species richness, hotspots, and the scale dependence of range maps in ecology and conservation. *Proceedings of the National Academy of Sciences*, *104*, 13384–13389.

Ilangakoon, N., Glenn, N., Schneider, F. D., Dashti, H., Hancock, S., Spaete, L., & Goulden, T. (). Spaceborne lidar reveals trends and patterns of functional diversity in a semi-arid ecosystem, . (p. in review).

Isbell, F., Gonzalez, A., Loreau, M., Cowles, J., Díaz, S., Hector, A., Mace, G. M., Wardle, D. A., O'Connor, M. I., Duffy, J. E., Turnbull, L. A., Thompson, P. L., & Larigauderie, A. (2017). Linking the influence and dependence of people on biodiversity across scales. *Nature*, *546*, 65–72.

Jarzyna, M. A., & Jetz, W. (2018). Taxonomic and functional diversity change is scale dependent. *Nature Communications*, *9*.

Jetz, W., Cavender-Bares, J., Pavlick, R., Schimel, D., Davis, F. W., Asner, G. P., Guralnick, R., Kattge, J., Latimer, A. M., Moorcroft, P., Schaepman, M. E., Schildhauer, M. P., Schneider, F. D., Schrodt, F., Stahl, U., & Ustin, S. L. (2016). Monitoring plant functional diversity from space. *Nature Plants*, *2*, 16024.

Jones, K. R., Allan, J. R., Maxwell, S. L., Fuller, R. A., Venter, O., Watson, J. E. M., & Negret, P. J. (2018). One-third of global protected land is under intense human pressure. *Science*, *360*, 788–791.

Jucker, T., Bongalov, B., Burslem, D. F. R. P., Nilus, R., Dalponte, M., Lewis, S. L., Phillips, O. L., Qie, L., & Coomes, D. A. (2018). Topography shapes the structure, composition and function of tropical forest landscapes. *Ecology Letters*, (p. DOI: 10.1111/ele.12964).

Kunstler, G., Falster, D., Coomes, D. A., Hui, F., Kooyman, R. M., Laughlin, D. C., Poorter, L., Vanderwel, M., Vieilledent, G., Wright, S. J., Aiba, M., Baraloto, C., Caspersen, J., Cornelissen, J. H. C., Gourlet-Fleury, S., Hanewinkel, M., Herault, B., Kattge, J., Kurokawa, H., Onoda, Y., Peñuelas, J., Poorter, H., Uriarte, M., Richardson, S., Ruiz-Benito, P., Sun, I.-F., Ståhl, G., Swenson, N. G., Thompson, J., Westerlund, B., Wirth, C., Zavala, M. A., Zeng, H., Zimmerman, J. K., Zimmermann, N. E., & Westoby, M. (2016). Plant functional traits have globally consistent effects on competition. *Nature*, *529*, 204–207.

Liang, J., Crowther, T. W., Picard, N., Wiser, S., Zhou, M., Alberti, G., Schulze, E.-D., McGuire, A. D., Bozzato, F., Pretzsch, H., De-Miguel, S., Paquette, A., Herault, B., Scherer-Lorenzen, M., Barrett, C. B., Glick, H. B., Hengeveld, G. M., Nabuurs, G.-J., Pfautsch, S., Viana, H., Vibrans, A. C., Ammer, C., Schall, P., Verbyla, D., Tchebakova, N., Fischer, M., Watson, J. V., Chen, H. Y. H., Lei, X., Schelhaas, M.-J., Lu, H., Gianelle, D., Parfenova, E. I., Salas, C., Lee, E., Lee, B., Kim, H. S., Bruelheide, H., Coomes, D. A., Piotto, D., Sunderland, T., Schmid, B., Gourlet-Fleury, S., Sonke, B., Tavani, R., Zhu, J., Brandl, S., Vayreda, J., Kitahara, F., Searle, E. B., Neldner, V. J., Ngugi, M. R., Baraloto, C., Frizzera, L., Ba azy, R., Oleksyn, J., A-Nied wiecki, T., Bouriaud, O., Bussotti, F., Finer, L., Jaroszewicz, B., Jucker, T., Valladares, F., Jagodzinski, A. M., Peri, P. L., Gonmadje, C., Marthy, W., OBrien, T., Martin, E. H., Marshall, A. R., Rovero, F., Bitariho, R., Niklaus, P. A., Alvarez-Loayza, P., Chamuya, N., Valencia, R., Mortier, F., Wortel, V., Engone-Obiang, N. L., Ferreira, L. V., Odeke, D. E., Vasquez, R. M., Lewis, S. L., Reich, P. B., Zawi a Nied wiecki, T., Bouriaud, O., Bussotti, F., Finer, L., Jaroszewicz, B., Jucker, T., Valladares, F., Jagodzinski, A. M., Peri, P. L., Gonmadje, C., Marthy, W., OBrien, T., Martin, E. H., Marshall, A. R., Rovero, F. et al. (2016). Positive biodiversity-productivity relationship predominant in global forests. *Science*, *354*, aaf8957–aaf8957.

Lohbeck, M., Poorter, L., Paz, H., Pla, L., van Breugel, M., Martínez-Ramos, M., & Bongers, F. (2012). Functional diversity changes during tropical forest succession. *Perspectives in Plant Ecology, Evolution and Systematics*, *14*, 89–96.

MacArthur, R. H., & MacArthur, J. W. (1961). On bird species diversity. *Ecology*, *42*, 595–599.

Mace, G. M., Barrett, M., Burgess, N. D., Cornell, S. E., Freeman, R., Grooten, M., & Purvis, A. (2018). Aiming higher to bend the curve of biodiversity loss. *Nature Sustainability*, *1*, 448–451.

Marselis, S. M., Tang, H., Armston, J., Abernethy, K., Alonso, A., Barbier, N., Bissiengou, P., Jeffery, K., Kenfack, D., Labrière, N., Lee, S.-K., Lewis, S. L., Memiaghe, H., Poulsen, J. R., White, L., & Dubayah, R. (2019). Exploring the relation between remotely sensed vertical canopy structure and tree species diversity in Gabon. *Environmental Research Letters*, *14*, 094013.

Marselis, S. M., Tang, H., Armston, J. D., Calders, K., Labrière, N., & Dubayah, R. (2018). Distinguishing vegetation types with airborne waveform lidar data in a tropical forest-savanna mosaic: A case study in Lopé National Park, Gabon. *Remote Sensing of Environment*, *216*, 626–634.

Mitchard, E. T. (2018). The tropical forest carbon cycle and climate change. *Nature*, *559*, 527–534.

Müller, J., Bae, S., Röder, J., Chao, A., & Didham, R. K. (2014). Airborne LiDAR reveals context dependence in the effects of canopy architecture on arthropod diversity. *Forest Ecology and Management*, *312*, 129–137.

Müller, J., & Brandl, R. (2009). Assessing biodiversity by remote sensing in mountainous terrain: The potential of LiDAR to predict forest beetle assemblages. *Journal of Applied Ecology*, *46*, 897–905.

Müller, J., Stadler, J., & Brandl, R. (2010). Composition versus physiognomy of vegetation as predictors of bird assemblages: The role of lidar. *Remote Sensing of Environment*, *114*, 490–495.

Næsset, E., & Økland, T. (2002). Estimating tree height and tree crown properties using airborne scanning laser in a boreal nature reserve. *Remote Sensing of Environment*, *79*, 105–115.

Neuenschwander, A., & Pitts, K. (2019). The ATL08 land and vegetation product for the ICESat-2 Mission. *Remote Sensing of Environment*, *221*, 247–259.

O'Connor, B., Secades, C., Penner, J., Sonnenschein, R., Skidmore, A., Burgess, N. D., & Hutton, J. M. (2015). Earth observation as a tool for tracking progress towards the Aichi Biodiversity Targets. *Remote Sensing in Ecology and Conservation*, *1*, 19–28.

Petchey, O. L., & Gaston, K. J. (2006). Functional diversity: back to basics and looking forward. *Ecology Letters*, *9*, 741–758.

Pollock, L. J., Thuiller, W., & Jetz, W. (2017). Large conservation gains possible for global biodiversity facets. *Nature*, *546*, 141–144.

Randin, C. F., Ashcroft, M. B., Bolliger, J., Cavender-bares, J., Coops, N. C., Dullinger, S., Dirnböck, T., Eckert, S., Ellis, E., Fernández, N., Giuliani, G., Guisan, A., Jetz, W., Joost, S., Karger, D., Lembrechts, J., Lenoir, J., Luoto, M., Morin, X., Price, B., Rocchini, D., Schaepman, M., Schmid, B., Verburg, P., Wilson, A., Woodcock, P., Yoccoz, N., & Payne, D. (2020). Monitoring biodiversity in the Anthropocene using remote sensing in species distribution models. *Remote Sensing of Environment*, *239*, 111626.

Rödig, E., Cuntz, M., Rammig, A., Fischer, R., Taubert, F., & Huth, A. (2018). The importance of forest structure for carbon flux estimates in the Amazon rainforest. *Environmental Research Letters*, .

Roscher, C., Schumacher, J., Gubsch, M., Lipowsky, A., Weigelt, A., Buchmann, N., Schmid, B., & Schulze, E. D. (2012). Using plant functional traits to explain diversity-productivity relationships. *PLoS ONE*, *7*.

Sandel, B., Gutiérrez, A. G., Reich, P. B., Schrodt, F., Dickie, J., & Kattge, J. (2015). Estimating the missing species bias in plant trait measurements. *Journal of Vegetation Science*, *26*, 828–838.

Schimel, D., Pavlick, R., Fisher, J. B., Asner, G. P., Saatchi, S., Townsend, P., Miller, C., Frankenberg, C., Hibbard, K., & Cox, P. (2015). Observing terrestrial ecosystems and the carbon cycle from space. *Global Change Biology*, *21*, 1762–1776.

Schimel, D., Schneider, F. D., Participants, J. C., & Ecosystem (2019). Flux towers in the sky: global ecology from space. *New Phytologist*, *224*, 570–584.

Schneider, F. D., Leiterer, R., Morsdorf, F., Gastellu-Etchegorry, J.-P., Lauret, N., Pfeifer, N., & Schaepman, M. E. (2014). Simulating imaging spectrometer data: 3D forest modeling based on LiDAR and in situ data. *Remote Sensing of Environment*, *152*, 235–250.

Schneider, F. D., Morsdorf, F., Schmid, B., Petchey, O. L., Hueni, A., Schimel, D. S., & Schaepman, M. E. (2017). Mapping functional diversity from remotely sensed morphological and physiological forest traits. *Nature Communications*, *8*.

Seavy, N. E., Viers, J. H., & Wood, J. K. (2009). Riparian bird response to vegetation structure: a multiscale analysis using LiDAR measurements of canopy height. *Ecological Applications*, *19*, 1848–1857.

Simonson, W. D., Allen, H. D., & Coomes, D. A. (2014). Applications of airborne lidar for the assessment of animal species diversity. *Methods in Ecology and Evolution*, *5*, 719–729.

Skidmore, A. K., Pettorelli, N., Coops, N. C., Geller, G. N., Hansen, M., Lucas, R., Mücher, C. A., O'Connor, B., Paganini, M., Pereira, H. M., Schaepman, M. E., Turner, W., Wang, T., & Wegmann, M. (2015). Environmental science: Agree on biodiversity metrics to track from space. *Nature*, *523*, 403–405.

Stavros, E. N., Schimel, D., Pavlick, R., Serbin, S., Swann, A., Duncanson, L., Fisher, J. B., Fassnacht, F., Ustin, S., Dubayah, R., Schweiger, A., Wennberg, P., Stavros, N., Schimel, D., Pavlick, R., Serbin, S., Swann, A., Duncanson, L., Fisher, J. B., Fassnacht, F., Ustin, S., Dubayah, R., Schweiger, A., & Wennberg, P. (2017). ISS observations offer insights into plant function. *Nature Ecology & Evolution*, *1*, 1–4.

Title, P. O., & Bemmels, J. B. (2018). ENVIREM: an expanded set of bioclimatic and topographic variables increases flexibility and improves performance of ecological niche modeling. *Ecography*, *41*, 291–307.

Vierling, K. T., Vierling, L. A., Gould, W. A., Martinuzzi, S., & Clawges, R. M. (2008). Lidar: Shedding new light on habitat characterization and modeling. *Frontiers in Ecology and the Environment*, *6*, 90–98.

Violle, C., Navas, M.-L. L., Vile, D., Kazakou, E., Fortunel, C., Hummel, I., & Garnier, E. (2007). Let the concept of trait be functional! *Oikos*, *116*, 882–892.

Wathen, S., Thorne, J. H., Holguin, A., & Schwartz, M. W. (2014). Estimating the Spatial and Temporal Distribution of Species Richness within Sequoia and Kings Canyon National Parks. *PLoS ONE*, *9*, e112465.

Wehr, A., & Lohr, U. (1999). Airborne laser scanning—an introduction and overview. *ISPRS Journal of Photogrammetry and Remote Sensing*, *54*, 68–82.

Williams, L. J., Paquette, A., Cavender-Bares, J., Messier, C., & Reich, P. B. (2017). Spatial complementarity in tree crowns explains overyielding in species mixtures. *Nature Ecology & Evolution*, *1*, 63.

Wilson, A. M., & Jetz, W. (2016). Remotely Sensed High-Resolution Global Cloud Dynamics for Predicting Ecosystem and Biodiversity Distributions. *PLoS Biology*, *14*, 1–20.

Wright, I. J., Westoby, M., Reich, P. B., Oleksyn, J., Ackerly, D. D., Baruch, Z., Bongers, F., Cavender-Bares, J., Chapin, T., Cornellissen, J. H. C., Diemer, M., Flexas, J., Gulias, J., Garnier, E., Navas, M. L., Roumet, C., Groom, P. K., Lamont, B. B., Hikosaka, K., Lee, T., Lee, W., Lusk, C., Midgley, J. J., Niinemets, Ü., Osada, H., Poorter, H., Pool, P., Veneklaas, E. J., Prior, L., Pyankov, V. I., Thomas, S. C., Tjoelker, M. G., & Villar, R. (2004). The worldwide leaf economics spectrum. *Nature*, *428*, 821–827.

Zellweger, F., Roth, T., Bugmann, H., & Bollmann, K. (2017). Beta diversity of plants, birds and butterflies is closely associated with climate and habitat structure. *Global Ecology and Biogeography*, *26*, 898–906.

Zhao, F., Sweitzer, R. A., Guo, Q., & Kelly, M. (2012). Characterizing habitats associated with fisher den structures in the Southern Sierra Nevada, California using discrete return lidar. *Forest Ecology and Management*, *280*, 112–119.

Zhu, L., Fu, B., Zhu, H., Wang, C., Jiao, L., & Zhou, J. (2017). Trait choice profoundly affected the ecological conclusions drawn from functional diversity measures. *Scientific Reports*, *7*, 3643.